Available online at www.sciencedirect.com
SCIENCE DIRECT®
International Journal of Machine Tools & Manufacture 44 (2004) 637–647
INTERNATIONAL JOURNAL OF MACHINE TOOLS & MANUFACTURE DESIGN, RESEARCH AND APPLICATION
www.elsevier.com/locate/ijmactool

The assessment of cutting tool wear

Viktor P. Astakhov *

Astakhov Tool Service, 3319 Fulham Dr., Rochester Hills, MI 48309, USA

Received 1 August 2003; received in revised form 5 November 2003; accepted 25 November 2003

Abstract

Flank wear of cutting tools is often selected as the tool life criterion because it determines the diametric accuracy of machining, its stability and reliability. This paper argues that the existing criteria of flank wear are insufficient for its proper characterization. Their existence is due to the lack of knowledge on the contact conditions at the tool flank–workpiece interface. Known attempts to evaluate the physical processes at this interface do not help to resolve this issue. This paper compares different characteristics of the evaluation of flank wear. The contact process at the mentioned interface is analyzed through the experimental assessment of the contact stresses, and the full validity of Makarow's law is confirmed, i.e. minimum tool wear occurs at the optimum cutting speed. A new concept of tool resources is proposed and discussed. This resource is defined as the limiting amount of energy that can be transmitted through the cutting wedge until it fails.

1. Introduction

The contact phenomena on the tool flank surface are of interest because understanding them allows the explanation of tool flank wear and the formation of surface integrity of machined surfaces on workpieces. Nevertheless, there are few known studies available on the subject. Surprisingly, modern books on metal cutting do not consider these phenomena [1–7]. Flank wear is considered using an aged Taylor's tool life equation having a phenomenological nature.

According to the ANSI/ASME B94.55M-1985 standard [8], the assessment of flank wear is accomplished by its direct measurement. As suggested, the major cutting edge is divided into three zones, as shown in Fig. 1, for the purpose of the wear measurements: (1) Zone C is the curved part of the cutting edge at the tool corner, (2) Zone N is the quarter of the worn cutting edge length b_w farthest from the tool corner, (3) Zone B is the remaining straight part of the cutting edge between Zone C and Zone N. As such, the following criteria for carbide tools are normally recommended: (a) the average width of the flank wear land $VB_B = 0.3$ mm, if the flank wear land is considered to be regularly worn in Zone B; (b) the maximum width of the flank wear land $VB_B max = 0.6$ mm, if the flank wear land is not considered to be regularly worn in Zone B. Besides, surface roughness for finish turning and the length of the wear notch $VB_N = 1$ mm can be used. However, these assessments are subjective and insufficient. They do not account for the tool geometry (the flank angle, the rake angle, the cutting edge angle, etc.) so they are not suitable to compare cutting tools having different geometries. They do not account for the cutting regime and thus do not reflect the real amount of work material removed by the tool during the time over which the measured flank wear is achieved.

Another way to look at the problem is to understand the physical processes taking place at the tool–workpiece interface, called the flank contact area. As known [9], the contact processes on the tool flank are determined by the normal and frictional forces on the tool flank acting at the tool–workpiece interface. Due to complexity of the contact process on this interface, the ratio of the normal and contact forces does not follow those obtained in standard mechanical tests. These processes include severe friction and plastic deformation of the machined surface.

* Tel: +1-248-852-0246; fax: +1-253-563-7501.
E-mail address: astvik@lycos.com (V.P. Astakhov).
URL://gundrilling.tripod.com (V.P. Astakhov).

0890-6955/$ - see front matter © 2003 Elsevier Ltd. All rights reserved.
doi:10.1016/j.ijmachtools.2003.11.006

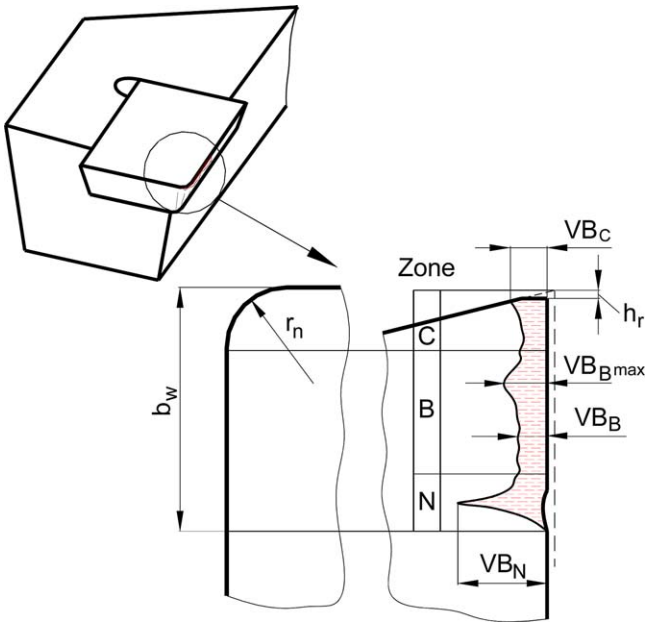

Fig. 1. Flank wear characteristics according to ANSI/ASME B94.55M-1985 standard.

The analysis of the attempts to derive an analytical expression for the flank forces is presented by Zorev [9]. He came to the surprising conclusion that if flank wear is small, the depth of cut is great, and workpiece hardness is "moderate", then the forces on the flank may not be taken into consideration because they are small in comparison with those on the rake face. On the contrary, if flank wear is large, and the depth of cut is small, particularly when machining hard materials, the flank forces become comparable with the forces on the tool rake. As such, the normal force on the flank face of the major cutting edge can be calculated as

$$N_f = q_{e\text{–}f}\frac{d_w}{\sin\kappa_r}h_f \approx \frac{\mathrm{HB}}{3}\frac{d_w}{\sin\kappa_r}h_f \quad (\mathrm{kg/mm^2}) \tag{1}$$

The friction force on this face is calculated as

$$F_f = \mu_{ff}q_{e\text{–}f}\left(\frac{d_w}{\sin\kappa_r}+f\right) \approx 0.2\mathrm{HB}\left(\frac{d_w}{\sin\kappa_r}+f\right) \quad (\mathrm{kg/mm^2}) \tag{2}$$

and the normal force on the flank surface of the minor cutting edge is calculated as

$$N_f = \frac{\mathrm{HB}}{3}fh_{f1} \quad (\mathrm{kg/mm^2}) \tag{3}$$

where d_w is the depth of cut, HB is the Brinell hardness of the work material, h_f and h_{f1} are the widths of the flank contact surfaces of the major and minor cutting edges, respectively, f is the cutting feed per revolution, and κ_r is the tool cutting edge angle.

Analyzing Eqs. (1)–(3), one can see that the distribution of the normal, $q_{e\text{–}f}$, and shear, $q_{s\text{–}f}$, stresses on the flank face contact area are assumed to be uniform. As such,

$$q_{e\text{–}f} \approx \frac{\mathrm{HB}}{3} \approx \sigma_{\mathrm{uts}} \quad (\mathrm{kg/mm^2}) \quad \text{and}$$
$$q_{s\text{–}f} \approx 0.2\mathrm{HB} \approx 0.6\sigma_{\mathrm{uts}} \quad (\mathrm{kg/mm^2}) \tag{4}$$

Moreover, these stresses do not depend on the cutting regime and tool material. Having noticed this fact, Zorev carried out a great number of cutting tests to establish the above-mentioned dependences. More than 20 different work materials having hardness from HB 80 (annealed pure iron) to HRC 65 (quench-hardened steel) were tested.

Fig. 2 shows the experimental results for cutting speeds that correspond to 90-min tool life. In Zorev's opinion, the reduction of $q_{e\text{–}f}$ while decreasing the cutting speed is attributed to the "secondary shear" on the rake face, which protects the flank contact surface. The same explanation is provided for the influence of the depth of cut d_w: if tool life is kept constant, the cutting speed decreases as the depth of cut increases. This statement is, however, in direct contradiction with Zorev's experiments on tool life (criterion—the width of the flank wear land), where increased cutting speed resulted in higher tool life. In other words, it should be recognized that something else, besides the stresses on the flank contact face, causes tool wear, and this "something" has not been reported as yet in previous papers on metal cutting.

As known [9,10], when the depth of cut becomes shallow, the nose radius of the cutting tool (or of the cutting insert used) plays an important role. As such, as seen from Fig. 2, the contact stress $q_{e\text{–}f}$ well exceeds the ultimate tensile strength of the work materials used in the tests. Because this is hardly possible, these high

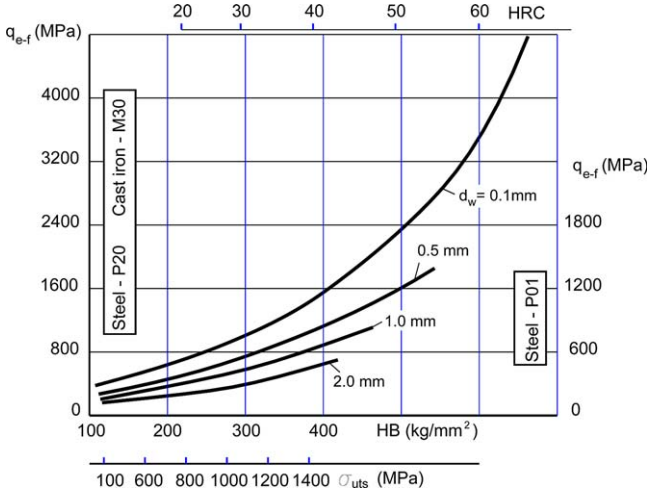

Fig. 2. Contact stresses at the tool flank according to Zorev.

stresses can be attributed to the irrelevant methodology of the flank contact stress determination for shallow depth of cut when the so-called nose effect is significant.

Another important experimental fact should be noted in Fig. 2, namely, the influence of the tool material. For the same tool life, the contact stress q_{e-f} and thus the forces on the flank contact face for the less wear resistant carbide P01 are approximately 25% lower than for more wear resistant P20 carbide. Nevertheless, Zorev recommended using the same apparent coefficient of friction $\mu_{ff} = 0.6$ for calculating the flank frictional force.

The objective of this paper is to compare different metrics for the assessment of tool wear, explain the physical background of the optimal cutting speed, and introduce a new concept of the resource of cutting tools.

2. Proper assessment of tool wear

The proper assessment of tool wear requires some quantitative characteristics. The selection of these characteristics depends upon a particular objective of a tool wear study. Most often, dimensional accuracy dictates this selection, i.e. the need to manufacture parts within the tolerance limits assigned for tool wear. As such, the tool life defined by this criterion may be referred to as dimension tool life. Dimension tool life can be characterized by the time within which the tool works without adjustment or replacement (T_{c-l}); by the number of parts produced (N_{p-l}); by the length of the tool path (L_{c-l}); by the area of the machined surface (A_{c-l}) and by the linear relative wear (h_{l-r}). All these characteristics listed are particulars and thus, in general, do not allow the optimal control of cutting operations, comparison of different cutting regimes, assessment of different tool materials, etc. For example, dimensional tool life is of little help if one needs to compare cutting tools that work at different cutting speeds and feeds and/or when the widths of their flank wear land are not the same. The dimensional wear rate, the relative surface wear and the specific dimensional tool life are much more general characteristics [10] to be used in metal cutting tests conducted everywhere from the research laboratory to shop floor level.

The dimension wear rate is the rate of shortening of the cutting tip in the direction perpendicular to the machined surface taken within the normal wear period, i.e.

$$v_h = \frac{dv_r}{dT} = \frac{h_r - h_{r-i}}{T - T_i} = \frac{vh_{l-r}}{1000} = \frac{vfh_s}{100} \quad (\mu m/min) \qquad (5)$$

where h_r and h_{r-i} are the current and initial radial wear, respectively; T and T_i are the total and initial operational time, respectively; h_s is the relative surface wear.

As follows from Eq. (5), the dimension wear rate is inversely proportional to tool life and does not depend on the selected wear criterion (a particular width of the flank wear land, for example).

The relative surface wear is the radial wear per 1000 sm^2 of the machined surface

$$h_s = \frac{dh_r}{dS} = \frac{(h_r - h_{r-i})100}{(l - l_i)f} \quad (\mu m/10^3\ sm^2) \qquad (6)$$

where h_{r-I} and l_i are the initial radial wear and initial machined length; l is the total machined length.

As follows from Eq. (6), the relative surface wear is inversely proportional to the overall machined area and, in contrast to it, does not depend on the selected wear criterion.

The specific dimension tool life is the area of the workpiece machined by the tool per 1 μm of its radial wear

$$T_{UD} = \frac{dS}{dh_r} = \frac{1}{h_s} = \frac{(l - l_i)f}{(h_r - h_{r-i})100} \quad (10^3\ sm^2/\mu m) \qquad (7)$$

The relative surface wear and the unit dimension tool life are versatile tool wear characteristics because they allow comparison of different tool materials for different combinations of cutting speeds and feeds for different selected criteria for tool life. Table 1 presents a comparison of different assessments of tool wear and thus tool life.

It is also possible to use the width of the wear land at the tool point (nose) (current VB_C and initial VB_{C-i}) instead of the radial wear (Fig. 1), i.e.

$$h_s = \frac{(VB_C - VB_{C-i})100}{(l - l_i)f} \quad (\mu m/10^3\ sm^2) \qquad (8)$$

Although such a substitution is correct, it is difficult to correlate VB_C with the dimensional accuracy of machining. This is due to the plastic lowering of the cutting edge which often occurs when machining difficult-to-machine materials.

3. Plastic lowering of the cutting edge

Normally, abrasion, adhesion, diffusion and oxidation types of cutting tool wear are discussed in literature on metal cutting. However, in the machining of difficult-to-machine materials and in high speed machining, plastic lowering of the cutting edge is the predominant cause of premature tool failure. This is due to the plastic deformation of the cutting wedge (a part of the tool between the rake and the flank contact surfaces). Fig. 3 illustrates the result of plastic deformation (known as lowering) of the cutting wedge. As seen, the rake, γ, and flank, α, angles change due to

Table 1
Comparison of different characterizations of tool life

Characteristic	Designation/equation	Restriction factors				Possibility of use in calculations of dimension accuracy
		Cutting speed, v (m/min)	Cutting feed, f (mm/rev)	Dimensions of the machined part (surface)	Tool wear VB_m or WB_r	
Machining time without adjustment or replacement of the tool, min	T_{c-l}	+	+	−	+	No
Number of parts produced without adjustment or replacement of the tool	N_{p-l}	−	−	+	+	No
Length of the tool path	$L_{c-l} = vT_{c-l}$	−	+	−	+	No
Area of the machined surface	$A_{c-l} = 10vT_{c-l}f$	−	−	−	+	No
Linear relative wear	$h_{l-r} = \frac{(h_r - h_{r-i})1000}{(l-l_i)}$	−	+	−	−	Yes
Dimension wear rate	$v_h = \frac{vh_{l-r}}{1000}$	+	+	−	−	Yes
Relative surface wear	$h_s = \frac{(h_r - h_{r-i})100}{(l-l_i)f}$	−	−	−	−	Yes
Specific dimensional tool life	$T_{UD} = \frac{(l-l_i)f}{(h_r - h_{r-i})100}$	−	−	−	−	Yes

Note that "+" means that the restrictive factors should be kept the same when using this characteristic for the comparison of cutting tools and regimes.

plastic lowering h_r of the cutting edge. This lowering is characterized by three parameters, l_γ, l_α, and h_α, as seen in Fig. 3. When these parameters reach a certain limit, breakage of the cutting wedge takes place. To prevent this from happening, the transition surface between the rake and the frank surface is often made as a fillet or chamfer instead of a sharp cutting edge.

The primary cause of plastic lowering of the cutting wedge is high-temperature creep. It is known that when temperatures at the tool–chip interface reach 1000–1200 °C, the cutting wedge deforms plastically [9–12]. Creep is progressive deformation of a material at constant stress. The engineering creep curve shown in Fig. 4 represents the dependence of plastic deformation of a metal when constant load and temperature are applied. As seen, upon loading of a pre-heated specimen, deformation increases rapidly from zero to a certain value ε_0, known as initial rapid elongation [12]. There is no need for additional energy for this deformation because it occurs due to the thermal energy that already exists in the specimen, so the work done by the internal forces begins with the level of energy that has already been achieved. In other words, if the temperature is a characteristic of the thermal energy, and deformation and stress characterize the work done by the external forces, then the critical amount of

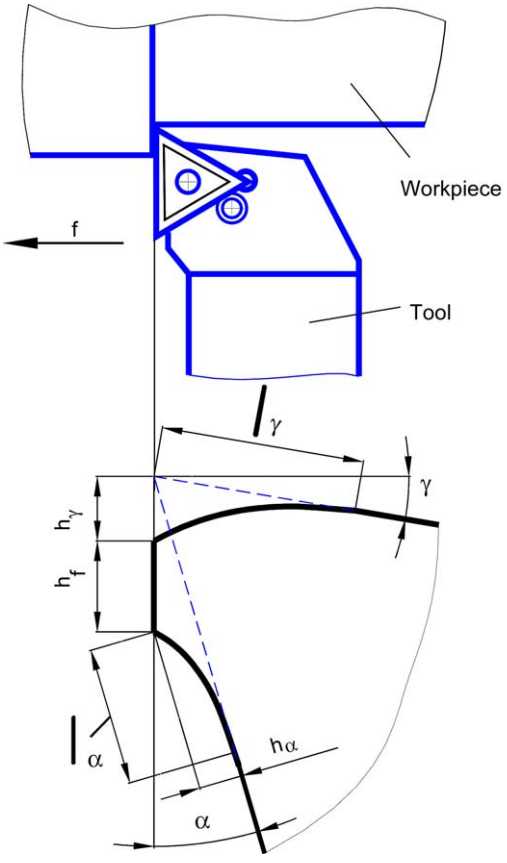

Fig. 3. Plastic lowering of the cutting edge.

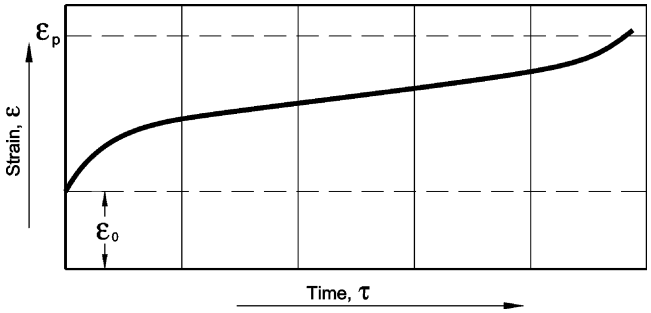

Fig. 4. Engineering creep curve.

energy accumulates in the material as the result of their summation.

Among the phases normally present in the sintered carbides used as the tool material, the plastic deformation is greater in the cobalt phase, as seen in Fig. 5, which generalizes the experimental results obtained by Makarow [10]. This plastic deformation results in tearing-off of the grains of carbide from deforming cobalt layers, "ploughing" this deforming layer by hard inclusions contacting the work material, and "spreading" of the tool material on the chip and workpiece contact surfaces. If the temperature increases further, a liquid layer forms between tool and workpiece due to diffusion, leading to the formation of the low-melting-point compound Fe_2W having melting temperature $T_m = 1130\ ^\circ C$. This layer is quickly removed in cutting [10].

The above-mentioned cause for the plastic lowering of the cutting edge at high temperatures has excellent experimental confirmation, known (but not explained) in everyday machining practice. Although fine grain carbides are superior to those having coarse grains in terms of wear resistance, coarse grain carbides, having higher creep resistance, exhibit much smaller plastic lowering of the cutting edge under the same cutting conditions.

4. Physical criterion of minimal tool wear

Probably the greatest advancement in the consideration of tool wear in machining was made by Makarow [10,11], who for the first time considered various interrelationships among cutting phenomena. On the basis of his findings, he formulated the law which was presented as the first metal cutting law (Makarow's law) by Astakhov [11]: for a given combination of tool and workpiece materials, there is a cutting temperature, referred to as the optimum cutting temperature θ_{opt}, at which the combination of minimum tool wear, minimum stabilized cutting force, and highest quality of the machined surface is achieved. This temperature is invariant to the way it has been achieved (whether the workpiece was cooled, pre-heated, etc.).

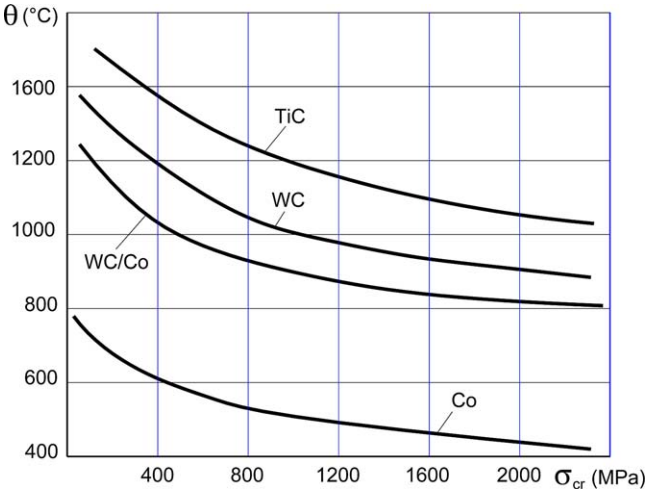

Fig. 5. Creep resistance of different phases of carbides.

As well known [10,11], the cutting speed has a direct and very strong influence on the cutting temperature. This fact allowed Makarow [10] to introduce the concept of optimal cutting speed, v_{opt}, as that speed at which the optimum cutting temperature and thus the minimum tool wear is achieved. The optimum cutting speed, v_{opt} defining this criterion is the only technically sound objective parameter, because the other known optimum cutting speeds are determined using non-physical criteria such as highest productivity, minimum cost per part, etc., and thus are associated with organizational rather with technical conditions. The introduced parameter seems to be the only proper technical parameter to compare different tool designs, geometry and tool materials, different cutting regimes, and machinability of different work materials. For example, there is no other way to compare different tool materials available today because the answer to the simple question of how to compare different carbide grades does not exist. Should one compare them using the same cutting regime, which can be preferable for one grade and completely unacceptable for the other? If the comparison is carried out using different cutting regimes, then one should know how to compare the results obtained.

To obtain an idea about the physical process at the flank–workpiece interface, the forces acting on this flank should be considered. The normal force is the result of the work material resistance to tool penetration into the workpiece. This force depends upon the compression yield strength of the surface layer of the work material, tool–workpiece contact area, and curvature of the edges of the flank wear land. The normal force defines the normal stress at the tool–workpiece interface and, through the apparent friction coefficient, the tangential force and shear stress distribution on this interface.

The properties of the work and tool materials, and tool geometry, as well as the cutting regime, determine the contact phenomena of the tool–workpiece interface. As such, the cutting speed has the strongest influence [9,11]. However, this influence is not obvious. To clarify the issue, a series of turning tests were carried out.

Since the outcomes of the metal cutting process are known to be very sensitive to relatively small changes in the cutting parameters [11], special attention was paid to the selection of the conditions of the tests and to the experimental methodology. The test conditions were selected as follows:

(1) *Workpiece material*: The water-hardened carbon–chromium tool steel W5 and nickel-based superalloy Inconel 718 were selected for the present study. The composition (the element limits) were selected according to the requirements of standard ANSI/ASME B94.55M-1985 and were requested from the steel dealer. The actual chemical composition has been analyzed using a LECO® SA-2000 Discharge-Optical Emission Spectrometer. The results were compared with those obtained from the dealer. The actual chemical composition and relevant mechanical properties were:

- Steel W5: 97%Fe, 1.12%C, 0.24%Si, 0.48%Cr, 0,25%Mn, 0.015%P, 0.024%S, 1.03%Cr, 0.16% Mo. The hardness was 270HB. Tensile strength, ultimate—920 MPa, tensile strength, yield—455 MPa.
- Superalloy Inconel 718: 0.05%C, 53%Ni, 18%Cr, 2.40%Ti, 1.20%Nb + Ta, 0.5%Al, 2.8%Mo, 0.34 %Si, 0.35%Mn, 0.29%Cu. Tensile strength, ultimate—1140 MPa, tensile strength, yield—414 MPa.

Before testing, hardness has been determined over the complete cross section of the terminal end and working length of each bar workpiece used in the tests. Cutting tests were conducted only on the bars where the hardness was within the limits ±10%. Special metallurgical parameters such as the element counts, microstructure, grain size, inclusions count, etc. were inspected using quantitative metallography.

(2) *Machine*: A retrofitted Schaerer HPD 631 lathe was used. The drive unit motor was replaced with a 15 kW variable speed AC motor and the feed motor was replaced with a 5 kW variable speed AC motor. The motors were individually controlled by AC invertors. The AC invertors are designed to provide the required volts/hertz ratio, allowing the AC motors to run at their optimum efficiency and provide rated torque capability through the motor's rated base speed. The control section of the AC invertors consists of a control board with a 16-bit microprocessor and keypad interface with an 8-bit microprocessor.

(3) *Cutting tool*: A general purpose tool holder CTJNR2520L16 and cutting inserts made of P20 (8%Co, 15%TiC, 77%WC) general purpose carbide were used. The geometry parameters of the tool were controlled according to American National Standard B94.50-1975. Tolerances for all angles were $\pm 0.5^{\circ}$. The roughness R_a of the tool face and flank did not exceed 0.25 μm and was measured according to American National Standard ANSI B46.1-1978. Each cutting edge was examined at a magnification of 15× for visual defects such as chip or cracks.

The tool wear was measured using a toolmaker's microscope (equipped with a digital video system) according to standard ANSI/ASME B94.55M-1985. The test preparation procedure, number of repetitions, and evaluation of the test results were discussed earlier [13].

(4) *Dynamometer*: A 2-component Kistler Type 9271A dynamometer was used. Based on the standard mounting as specified by the supplier (Kistler), the load washer (Kistler Type 9065) was installed in the dynamometer and pre-loaded to 120 kN. At this pre-load, the range for force measurements is from −20 to +20 kN; threshold is 0.02 N; sensitivity is −1.8 pC/N; linearity does not exceed a range of ±1.0%FSO; overload is 144 kN; cross talk does not exceed 0.02 N/N; resonant frequency is 40 kHz; temperature error does not exceed +30 N/°C.

The load washer was connected to the charge amplifiers (Kistler, Mod. 5004). The charge amplifier (Type 5004) is a mains-operated DC amplifier of very high input impedance with capacitive negative feedback, intended to convert the electric charge from a piezoelectric transducer into a proportional voltage on the low impedance amplifier output. The calibration factor setting (adjustment of transducer sensitivity at the amplifier) makes standardized amplifier sensitivities of, for example, 1, 2, 5, etc. mV per mechanical unit (N) possible. The carefully designed calculating disc enables the reciprocal value of sensitivity to be shown directly as a measuring range.

Charge calibrators Type 541A were connected ins tead of transducers, allowing the entire measuring chain to be calibrated with an appropriate charge signal.

Cables used in the connections were specially made for Kistler equipment. In addition to an extremely high insulation resistance, they are free from disturbing charge signals when the cables are moved around. 1619 cables protected by metallic tubing were used.

The outputs of the charge amplifiers were connected to the FFT analyzer (B&K, Mod. 2032). The dual channel signal analyzer (Type 2032) is flexible, easy to use, and is a fully self-contained two-channel FFT analysis system with 801 lines of resolution. The analyzer has a real-time speed of >5 kHz (>10 kHz in single channel). This type of FFT analyzer was selected since it is flexible, i.e. calibration, display scales, post-processing, etc. are user-definable, and functions such as signal-to-noise ratio, cross-spectra, autospectra, etc. are computed directly without the need for intermediate processing. It is also easy to use because the operation has all relevant control settings clearly shown on

the display screen, and because complete measurement and display setups can be stored for later recall and use. The analyzer is self-contained because it has a fully instrumented front-end, built-in digital zoom, a built-in zooming signal generator and IEC/IEEE interface. Its 801-line resolution is of special importance since more modes of vibration can be identified and characterized in a signal analysis than with a conventional 250- or 400-line analyzer.

The experimental setup was calibrated statically and dynamically. The methodology and conditions were the same as discussed earlier in [14].

The experimental results obtained using different groups of work materials show that the influence of the cutting speed on the contact characteristic at the flank–workpiece interface cannot be generalized, as suggested by Zorev [9], because it differs considerably from one work material to another. To illustrate this point, Fig. 6 shows the dependences of the normal and shear stresses at the flank contact area in machining high carbon tool steel AISI W5, while Fig. 7 shows these stresses for a heat resistant nickel-based high alloy Inconel 718. As seen, the normal and shear stress distributions do not follow a similar trend for these materials. However, regardless of the differences in the values and trend of the normal and shear stresses, two important similarities can be observed:

- The minimum tool wear occurs at the optimum cutting speed v_{opt}.
- The apparent friction coefficient reaches its lowest value at this speed.

The observed phenomena have to be explained. As such, the known works on tool wear which try to fit Taylor's tool life equation are of little help simply

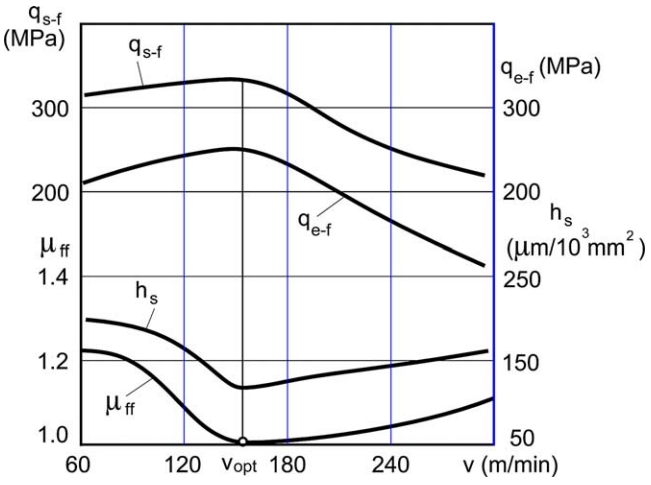

Fig. 6. Influence of the cutting speed on the normal ($q_{e\text{–}f}$), and shear, ($q_{s\text{–}f}$), stresses on at the flank contact area, and the apparent friction coefficient, μ_{ff}, in machining of high carbon tool steel AISI W5.

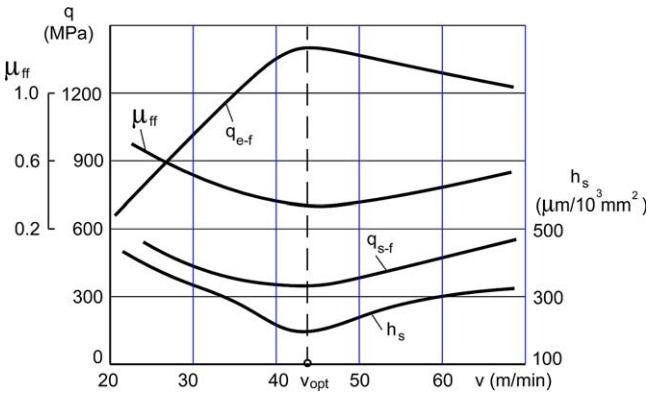

Fig. 7. Influence of cutting speed on the normal ($q_{e\text{–}f}$), and shear ($q_{s\text{–}f}$), stresses on at the flank contact area, and the apparent friction coefficient, μ_{ff}, in machining of Inconel 718.

because they do not consider the physics of metal cutting, trying to substitute this physics by phenomenological observations.

To explain the discussed phenomena, one should recognize that metal cutting is the purposeful fracture of the work material as defined by Astakhov [11]. The work spent in purposeful fracturing of the layer being removed, i.e. its fracture toughness, should be considered as the prime parameter in determining the cutting force and cutting energy. Therefore, one should consider the mechanics of fracture [15] and the importance of the process temperature in this mechanics. Another important aspect of metal cutting is plastic deformation, which should be considered as a waste of energy. In any other metal forming process, especially involving high strains (deep drawing, extrusion), plastic deformation is used to accomplish the process. Parts are formed into useful shapes such as tubes, rods, and sheets by displacing the material from one location to another. Therefore, better materials, from the viewpoint of metal forming, should exhibit higher strain before fracture occurs. It is understood that this is not the case in metal cutting, where it is desired that the work materials have the strain at fracture as small as possible.

According to Atkins and Mai [15] and Komarovsky and Astakhov [12], there is a marked increase in tensile strain to fracture, and also in the work of fracture, at about 0.018–0.25 of the melting point (T_m); similar changes occur in other measures of ductility such Charpy values (CVN), as shown in Fig. 8a. It explains a number of "strange" results obtained by Zorev in his tests at low cutting speeds [9]. This phenomenon also explains the great size of the zone of plastic deformation observed at low cutting speeds and incorporated in the model discussed by Astakhov [11]. The known built-up edge is the result of the discussed high plasticity region. Exceptions are certain fcc metals and alloys (Al, Cu, Ni, Pb) that do not normally cleave. As

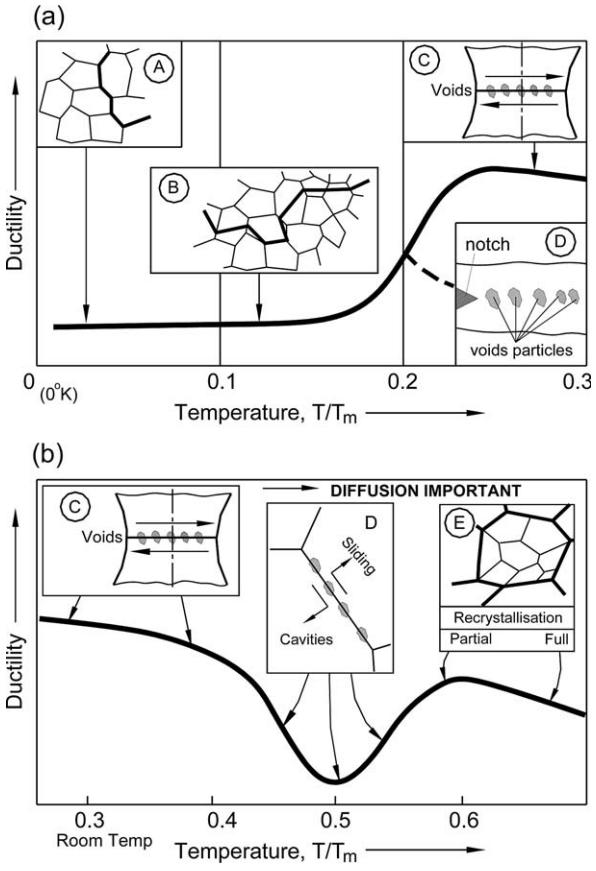

Fig. 8. Changes in ductility and typical associated mechanisms of fracture for bss materials: (a) at temperatures $<0.3T_m$: (A) low-temperature intergranular cracks, (B) twinning or slip leading to cleavage, (C) shear fracture at particles, (D) low energy shear at particles; (b) at temperatures $>0.3T_m$: (C) shear at particles, (D) cavities along grain faces, (E) re-crystallization suppresses cavitation.

such, there is no transition in values, which gradually rise with temperature.

The increase in ductility over the "transition temperature range" is followed by a gradual drop beyond approximately $0.35T_{\mathrm{m}}$. It is believed that it happens due to the continuing fall in the Pierls–Nabarro stress which opposes dislocation movement, coupled with the emergence of cross-slip (as opposed to Frank–Read sources) as a dislocation generator as the temperature is raised [15]. In the author's opinion, the cause is in dilations–compressions reactions, as explained in [12].

At high temperatures, the influence of grain boundaries become significant. Below approximately $0.45T_m$, grain boundaries act principally as barriers inhibiting cleavage and causing dislocation pile-ups. At higher temperatures, the regions of intense deformation, which are contained within the grains at lower temperatures, now shift to the grain boundaries themselves. Voids are nucleated and cracks then develop on the grain boundaries. Shear stresses on the boundaries cause relative sliding of the grains, and voids are reduced in regions of stress concentrations (see Fig. 8b—position D). Therefore, around this temperature region can be referred as *the ductility valley*. Experiments showed [10] that the reduction of plasticity may be twofold and even more for high alloys. The presence of this valley is the physical cause of the existence of the optimum cutting temperature.

At temperatures $(0.5–0.6)T_m$, recovery and re-crystallization processes set in (recovery relates to a re-distribution of dislocation sources so that dislocation movement is easier, and in re-crystallization, the energy of dislocations generated during prior deformation is used to nucleate and grow new grains, thus effecting an annealed structure over a long time). The net effect is increased ductility, causing a bump on the ductility curve as shown in Fig. 8b.

5. Comparison of different tool materials

The question about the proper selection of type (grade) of tool material is often one of hardest questions that is posed and needs to be considered in the design and implementation of cutting tools. Although there are a number of mechanical characteristics available for each tool material, no information on the correlation of these characteristics and the cutting ability of a tool material is provided. Therefore, if one needs to compare different tool materials, one faces a number of tough questions, such as: "What is the cutting speed and feed to be used in the tests? Should these materials be tested at the same speed and feed? How to compare the test results obtained at different speeds and feeds?" Unfortunately, the answers to these important questions cannot be found in literature on metal cutting.

Different tool materials (grades) can be compared using: (1) the cutting speeds corresponding to the same tool life; (2) tool lives corresponding to the same cutting speed. As such, the optimum cutting speeds for each tool material are used corresponding to the minimum tool wear. The dimension wear rate (Eq. (5)) is used as the wear criterion in the following form:

$$v_h = \frac{\mathrm{d}v_r}{\mathrm{d}L} = \frac{h_r - h_{r-i}}{L - L_i} = \frac{h_r - h_{r-i}}{v_{\mathrm{opt}} T_r} = \frac{\omega_r}{v_{\mathrm{opt}}} \tag{9}$$

where L and L_i are the total and initial cutting length, respectively, so that $L - L_i = v_{\mathrm{opt}} T_r$, where T_r is radial tool life, i.e. the time over which the critical radial wear is achieved; $\omega_r = (h_r - h_{r-i})/T_r$ is the rate of radial wear.

It follows from Eq. (9) that the higher the optimum cutting speed and the lower the rate of radial wear, the better a tool material.

6. Resource of the cutting wedge

As shown by Astakhov [11], the energy flows to the zone of fracture of the layer being removed through the cutting wedge, defined as the part of the tool located between the rake and the flank contact areas. Out of three components of the cutting system, namely, the cutting tool, the chip and the workpiece [11], the only component that has an invariable mass of material and which is continuously loaded during the process is the cutting wedge. As such, the overall amount of energy which can be transmitted through this wedge is entirely determined by the physical and mechanical properties of the tool material.

On the contrary, the material of the chip is not subjected to the same external force because the chip is an ever grooving component, i.e. a new section is added to the chip during each cycle of chip formation [11], while "old" sections move out over the tool–chip interface and then leave the tool rake face and thus do not experience the external load. The same can be said about the workpiece, the volume and thus mass of which changes during the cutting process as well as the area of load application imposed by the cutting tool.

When the cutting wedge loses its cutting ability due to wear or plastic lowering of the cutting edge (creep), the work done by the external forces that cause such a failure is regarded as the critical work. For a given cutting wedge, this work (or energy) is a constant value. The resource of the cutting wedge, therefore, can be represented by this critical work [12]. It was established by Huq and Celis that direct correlation exists between wear and the dissipated energy in sliding contacts [16].

According to the principle of physical theory of reliability [12], each component of a system has its resource spent during operation time at a certain rate depending on the operating conditions. This principle is valid for a wide variety of operating conditions providing that changes from one operating regime to another do not lead to any structural changes in materials properties (reaching the critical temperatures, limiting loads, chemical transformations, etc.). As such, the resource of a cutting tool, r_{ct}, can be considered as a constant, which does not depend on any particular mode of its consumption, i.e.

$$r_{ct} = \int_0^{\tau_1} f(\tau,R_1)\mathrm{d}\tau = \int_0^{\tau_2} f(\tau,R_2)\mathrm{d}\tau \qquad (10)$$

where τ_1 and τ_2 are the total operating time at operating regimes R_1 and R_2, respectively, till the resource of the cutting tool is exhausted.

If the initial resource of the cutting tool is represented by the above discussed critical energy, the flow of energy through the cutting tool exhausts this resource. The amount of energy that flows through the cutting tool depends on the energy to fracture of the layer being removed, which, in turn, defines the total energy U_{cs} required by the cutting system to exist. Therefore, there should be a strong correlation between a parameter (or metric) characterizing the resource of the cutting tool (for example, flank wear $h_{v\text{–}f}$) and the total energy U_{cs}.

The second series of cutting tests were carried out to prove this hypothesis experimentally. The experimental setup and methodology were the same. The work material was steel AISI 52100: chemical composition—0.95%C, 1.5%Cr, 0.35%Mn, 0.25%Si; tensile strength, ultimate—689 MPa, tensile strength, yield—558 MPa, annealed at 780 °C to hardness 192HB. The cutting tool material was carbide P10 (cutting inserts SNMM120404).

The experimental results are shown in Table 2. As follows from this table, there is a very strong correlation, which does not depend on a particular cutting regime, cutting time and other parameters of the cutting process, between the total work required by the cutting system and the flank wear. Fig. 9 shows the correlation curve.

Table 2
Conditions of tests and experimental results

Test No.	Feed (mm/rev)	Depth of cut (mm)	Operating time (s)	Flank wear, VB (mm)	Energy of the cutting system (kJ)
1	0.07	0.1	8540	0.45	0.88
2	0.07	0.1	6680	0.41	0.63
3	0.07	0.1	4980	0.39	0.52
4	0.07	0.1	1640	0.29	0.25
5	0.07	0.1	9120	0.45	0.91
6	0.07	0.1	7660	0.42	0.68
7	0.07	0.1	6260	0.41	0.55
8	0.07	0.1	4900	0.37	0.41
9	0.07	0.1	3450	0.35	0.47
10	0.07	0.1	5380	0.38	0.65
11	0.07	0.1	4240	0.34	0.35
12	0.07	0.1	3150	0.30	0.33
13	0.07	0.1	2075	0.26	0.24
14	0.07	0.1	1036	0.20	0.15
15	0.07	0.1	2980	0.37	0.37
16	0.07	0.1	1940	0.32	0.30
17	0.07	0.1	1190	0.27	0.17
18	0.09	0.1	938	0.15	0.05
19	0.09	0.1	1874	0.18	0.10
20	0.09	0.1	2840	0.22	0.22
21	0.09	0.1	3820	0.25	0.17
22	0.09	0.1	4810	0.31	0.39
23	0.12	0.1	775	0.20	0.08
24	0.12	0.1	1520	0.23	0.18
25	0.12	0.1	2350	0.26	0.29
26	0.12	0.1	3220	0.27	0.30
27	0.14	0.1	675	0.20	0.18
28	0.14	0.1	1315	0.21	0.12
29	0.07	0.2	1295	0.21	0.13
30	0.07	0.2	2610	0.27	0.30
31	0.07	0.2	5420	0.44	0.82
32	0.07	0.8	1316	0.20	0.19

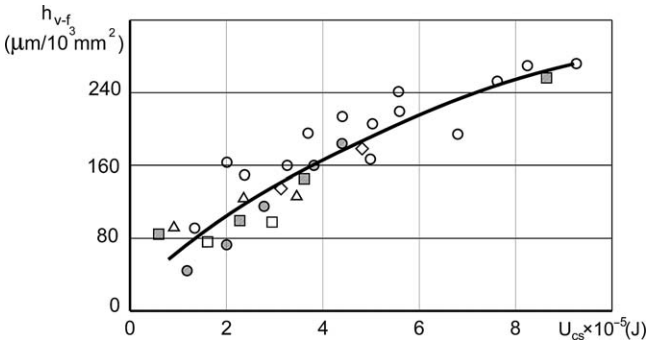

Fig. 9. Correlation curve.

The discovered correlation between the energy passed through the cutting wedge and its wear can be used for the predictions of tool life and optimum cutting speed, allowing the avoidance of expensive and time-consuming tool life tests. Moreover, the multiple experimental results, obtained in the machining of different work materials using different cutting tools, prove that this correlation holds regardless of the particular manner in which the resource of the tool was spent.

The essence of the method can be described as follows.

The energy required by the cutting system during the time period corresponding to tool life T_{ct} can be represented as

$$U_{cs} = W_{cs} T_{ct} \tag{11}$$

where W_{cs} is the power required by the cutting system (W). Note that U_{cs}, when selected for a given tool material using the correlation curve similar to that given in Fig. 9 for the accepted tool life criterion, is the sole characteristic of the tool material, i.e. its resource can be used for calculating tool life in cutting different work materials.

The power of the cutting system, W_{cs}, is determined as a product of the power component of the cutting force (often referred to as the cutting force), P_z, and the cutting speed, v, i.e.

$$W_{cs} = P_z v \tag{12}$$

In turn, the power component of the cutting force can be determined experimentally depending upon the cutting parameters as [14]

$$P_z = C_{P_z} d^{n_z} f^{m_z} v^{k_z} \tag{13}$$

where C_{P_z} is the constant of the work material, and n_z, m_z,k_z are exponents. Substituting Eqs. (12) and (13) into Eq. (11) and expressing tool life, one can obtain an equation which determines tool life for a given cutting regime:

$$T_{ct} = \frac{U_{cs}}{C_{P_z} d^{n_z} f^{m_z} v^{k_z+1}} \tag{14}$$

If it is necessary to know the cutting speed corresponding desired tool life, then Eq. (14) can be expressed as

$$v = \left(\frac{U_{cs}}{C_{P_z} d^{n_z} f^{m_z} T_{ct}} \right)^{1/(k_z+1)} \tag{15}$$

It is obvious that U_{cs} is selected depending on the tool flank wear, which depends not only on the properties of the tool material but also on the tool geometry. Therefore, the correlation curve $U_{cs} = f(\mathrm{VB})$ should be corrected accounting for the particular tool geometry. As a result, there are countless numbers of possible combinations of ''cutting tool material-tool geometry'' to account for the influence of the tool geometry. To avoid the influence of tool geometry, the volume of worn tool material, VW, can be used.

The results of the foregoing analysis suggest that the most prospective way to achieve repeatability of cutting tools with inserts is the certification of cutting inserts of standard shapes. The number of standard shapes of cutting inserts (including their geometry) is relatively small, so each insert producer should be able to provide a correlation curve $U = f(\mathrm{VB})$ for each shape and tool material. Table 3 presents some correlations for different tool materials and for different shapes of cutting inserts, obtained experimentally using basic groups of work material (low, medium and high carbon steels, low and high alloys including chromium and nickel based ones, titanium alloys). It has been proven that the correlation curves obtained do not depend on the particular work material, machine or any other cutting conditions, so they are sole properties of the considered tool materials.

Table 3
Correlation curves for some tool materials

Tool material	ISO code of the shape	Correlation curve	Critical temperature (°C)
TS332 (Al_2O_3, 2300HV)	SNMN 120404M	$U = \exp(9.6\mathrm{VB}^2)$	1200
VOK60 (Al_2O_3 + TiC 94 HRA)	SNMN 120404M	$U = \exp(10.91\mathrm{VB}^2)$	1200
Silinit-P ($Si_3N_4 + Al_2O_3$, 96 HRA)	SNMN 120404M	$U = 573\mathrm{VB}^2$	1200
TN20 (75%TiC, 15%Ni, 10%Co, 90HRA)	SNMN 120404M	$U = 434.46 \times 10^{-3}\mathrm{VB}^2$	780
Kiborit (96% cBN, KNH 32–36 GPa)	RNMM1200404M	$U = 50\mathrm{VB}^{1/2}$	1400

The correlation curves in this table were obtained for VB $\leq$ 0.4 mm. The data presented in Table 3 are valid under the condition that the tool material does not lose its cutting properties due to excessive temperature. For example, the data for Silinit-P are valid if the cutting temperature does not exceed that in cutting steel with feed $f = 0.07$ mm/rev, depth of cut $d = 0.1$ mm and cutting speed $v = 3.3$ m/s. If the cutting speed is increased to $v = 4$ m/s, this material loses its cutting ability, so the correlation curve presented in Table 3 is no longer valid.

7. Conclusions

The results of this paper can be summarized in the following conclusions:

- The existing metrics for tool wear are out of date because they cannot be used for the objective comparison of tool performance.
- Dimensional accuracy often dictates the selection of a tool wear criterion. As such, relative surface wear seems to be the most objective estimate for tool wear because it does not depend on the selected wear criterion.
- The properties of the work and tool materials, tool geometry and the cutting regime determine the contact phenomena of the tool–workpiece interface. As such, the cutting speed has the strongest influence. Regardless of the differences in the values and trends of the normal and shear stresses at the contact interfaces, minimum tool wear occurs and apparent friction coefficient reaches its lowest value at the optimum cutting speed v_{opt}. This is explained by the plasticity valley in the "ductility–temperature" dependency for most common work materials.
- In the machining of difficult-to-machine materials and in high speed machining, plastic lowering of the cutting edge is the predominant cause of premature tool breakage. This lowering is a result of high-temperature creep of the tool material.
- A new concept of resource of the cutting tool based upon the physical theory of reliability is presented. As such, this resource is defined as the limiting amount of energy that can be transmitted through the cutting wedge until it fails. It is shown that the resource of the cutting edge does not depend on a particular manner of exhaustion.

Acknowledgements

The assistance of Ms. Mary J. Silva in the preparation of the manuscript is gratefully acknowledged.

References

[1] M.C. Shaw, Metal Cutting Principles, Oxford Science Publications, Claredon Press, Oxford, 1984.
[2] F.Y. Gorczyca, Application of Metal Cutting Theory, Industrial Press, New York, 1987.
[3] P.L.B. Oxley, Mechanics of Machining: An Analytical Approach to Assessing Machinability, John Wiley & Sons, New York, USA, 1989.
[4] D.A. Stenphenson, J.S. Agapiou, Metal Cutting Theory and Practice, Marcel Dekker, 1996.
[5] Y. Altintas, Manufacturing Automation, Metal Cutting Mechanics, Machine Tool Vibrations, and CNC Design, Cambridge University Press, 2000.
[6] T.H.C. Childs, K. Maekawa, T. Obikawa, Y. Yamane, Metal Machining. Theory and Application, Arnold, London, 2000.
[7] E.M. Trent, P.K. Wright, Metal Cutting, fourth ed., Dutterworth-Heinemann, Boston, 2000.
[8] American National Standard "Tool Life Testing With Single-Point Turning Tools" ANSI/ASME B94.55M-1985", ASME, New York, 1985.
[9] N.N. Zorev, (M.C. Shaw, Trans.) Metal Cutting Mechanics, Pergamon Press, Oxford, 1966.
[10] A.D. Makarow, Optimization of Cutting Processes (in Russian), Mashinostroenie, Moscow, 1976.
[11] V.P. Astakhov, Metal Cutting Mechanics, CRC Press, Boca Raton, USA, 1998.
[12] A.A. Komarovsky, V.P. Astakhov, Physics of Strength and Fracture Control: Fundamentals of the Adaptation of Engineering Materials and Structures, CRC Press, Boca Raton, 2002.
[13] V.P. Astakhov, M.O.M. Osman, M. Al-Ata, Statistical design of experiments in metal cutting—part 1: methodology, Journal of Testing and Evaluation 25(3) (1997) 322–327.
[14] V.P. Astakhov, S.V. Shvets, A novel approach to operating force evaluation in high strain rate metal-deforming technological processes, Journal of Materials Processing Technology 117 (1–2) (2001) 226–237.
[15] A.G. Atkins, Y.W. Mai, Elastic and Plastic Fracture: Metals, Polymers. Ceramics, Composites, Biological Materials, John Wiley & Sons, New York, 1985.
[16] M.Z. Huq, J.-P. Celis, Expressing wear rate in sliding contacts based on dissipated energy, Wear 252 (2002) 375–383.